공학석사 학위논문

대기 중 수증기의 밀도 변화에 따른 THz 펄스의 시간 이동

The Time Shift of THz Pulse According to Water Vapor Density Variation in Atmosphere

지도교수 전태인

2018 년 02월

한국해양대학교 대학원

전기전자공학과

김 경 률

대기 중 수증기의 밀도 변화에 따른 THz 펄스의 시간 이동 측정

2018년 2월

김 경 률

공학석사 학위논문

대기 중 수증기의 밀도 변화에 따른 THz 펄스의 시간 이동

The Time Shift of THz Pulse According to Water Vapor Density Variation in Atmosphere

지도교수 전태인

2018 년 02월

한국해양대학교 대학원

전기전자공학과

김 경 률

본 논문을 김경률의 공학석사 학위논문으로 인준함.

위원장 장 낙 원 (인)

위 원 전 태 인 (인)

위 원 주 양 익 (인)

2017년 12월 04일

한국해양대학교 대학원

TABLE OF CONTENTS

List of Tables

List of Figures

대기 중 수증기의 밀도 변화에 따른 THz 펄스의 시간 이동

Kim, Gyeong Ryul

Department of Electrical and Electronics Engineering
Graduate School of Korea Maritime and Ocean University

Abstract

이 논문은 테라헤르츠 (THz) Time domain spectroscopy를 사용하여 대기중으로 186m와 910m 전파된 THz 펄스를 측정하였다. 186m와 910m 측정에서 외부 환경의 영향을 받은 거리는 각각 159m, 883m이며 거리가 늘어날수록 대기에 반응하는 시간이 길어지기 때문에 수분에 의한 흡수가 많이 일어나며 짧은 거리에서 보이지 않는 수분 공명을 확인할 수 있다.
수증기 밀도가 증가함에 따라 측정된 THz 펄스는 시간 지연이 발생하며 186m 측정보다 910m 측정이 더 많은 시간 지연을 가진다. 또한 대기에 의한 흡수 때문에 크기가 줄어들고 군속도 확산의 영향으로 펄스 모양이 넓게 퍼진다. 보다 정확한 측정을 위하여 주파수영역 위상 변이, 시간영역에서 시간 지연을 통해 Time shift를 비교하였다.
대기 환경의 변화를 대기 굴절률의 변화로 해석하여 Smith & Weintraub의 굴절률 공식으로 대기의 굴절률을 구하였다. 계산한 굴절률을 이용하여 THz 펄스의 시간이동을 예측할 수 있고 측정 데이터와 비교하였다.

KEY WORDS: Atmospheric propagation; Absorption; Spectroscopy, terahertz.

이러한 Water Vapor Density(WVD)에 따른 장거리 THz 연구는 대기에서의 THz 통신과 위험 가스 모니터링과 같은 응용분야에 사용될 가능성이 있다.

Chapter 1. Introduction

The Terahertz (THz) electromagnetic wave is a far-infrared region wave having a frequency of 0.1 THz to 10 THz. Therefore, it is possible to transmit a substance which can't be transmitted by light waves or radio waves, and has a nondestructive characteristic that does not destroy the transmitted substance due to low energy. Unlike the past, which has difficulties in generating THz electromagnetic waves, THz electromagnetic waves can be generated in various ways at present. Therefore, THz communication, bio sensing, imaging, and characterization can be studied and applied[1-8].

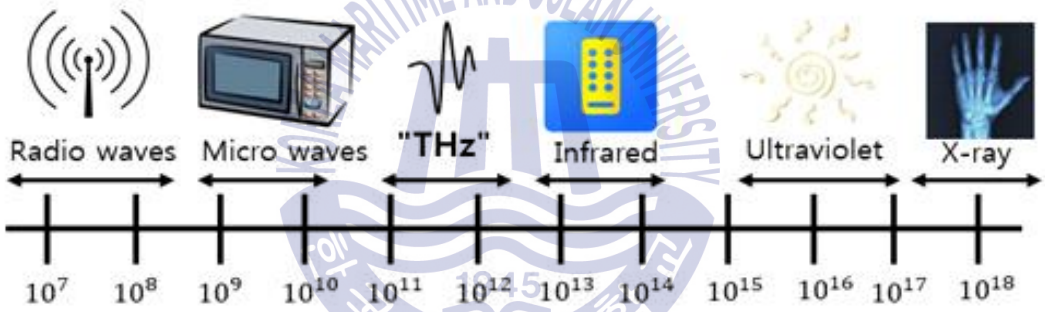

Figure 1-1 Electromagnetic wave spectrum

In recent years, much research has been conducted on THz communication as well as THz-Imaging. However, as with light waves, it is not easy to propagate to the atmosphere due to the high absorption rate by the atmosphere. Therefore, it was measured according to the change of the water vapor density(WVD) to see how the atmospheric moisture affects the THz electromagnetic wave. The density of water vapor is g/m^3 in terms of the amount of water vapor per unit volume and is a unit widely used in this paper. There is a group that has successfully propagated 167 meters indoors, and we have also succeeded in propagating 186 meters in the atmospheric in our laboratory[9-18]. In this paper, we have investigated the characteristics of

THz electromagnetic waves propagated by propagating 910m in the atmosphere by further increasing the distance.

Chapter 2. Experiment Setup

2.1 THz Generation and Detection

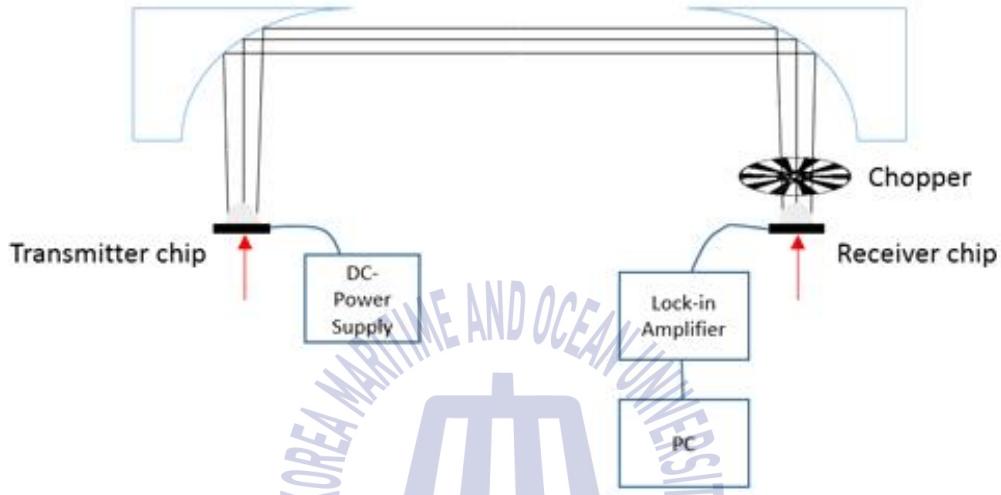

Figure 2-1 The schematic diagram of standard THz-TDS system

The most commonly used Terahertz Time-Domain Spectroscopy (THz-TDS) system is shown in figure 2-1[20]. The basic configuration of the experiment used in this paper and the reference pulse can be obtained. In order to generate THz electromagnetic wave, Mai-Tai (Wavelength: 790 nm, repetition rate: 84.01 MHz, pulse width: 50 fs) of Spectra-Physics Co., which is a laser with a narrow pulse width, is used. When the laser is incident on the transmitter chip (TX), Photo carriers are generated, and the generated photo carriers are spread randomly on the semiconductor substrate. If a strong magnetic field is formed on the semiconductor substrate, the photo carriers generated by the laser pulse will flow into the metal transmission line. At this time, THz electromagnetic wave is generated by the change of the formed current. The generated THz electromagnetic wave is transmitted to the

receiver chip (RX) through two parabolic mirrors. Likewise, a laser is incident on RX to generate a photo carrier. At this time, a current flow due to the force of the electric field of the electromagnetic wave. The generated current is measured using a lock-in amplifier and the data is stored in the PC.

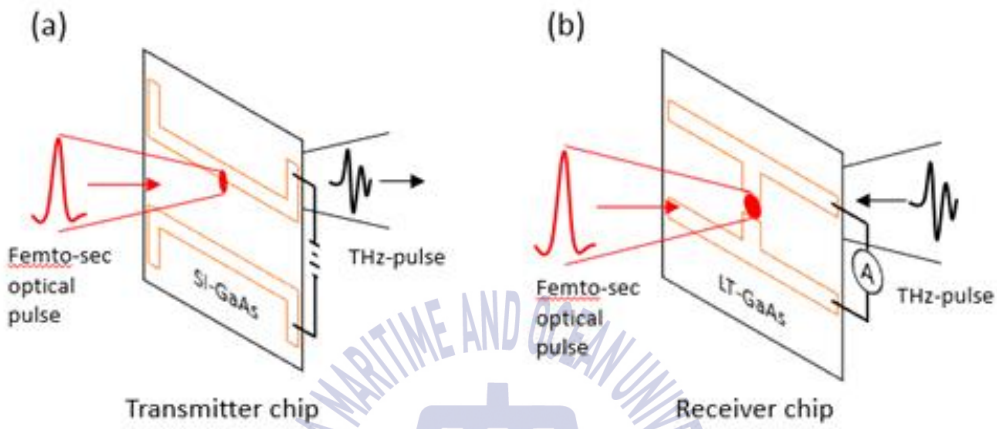

Figure 2-2 Used transmitter chip and receiver chip

Figure 2-2(a) is a schematic representation of a Transmitter chip and is a transmitter for generating THz electromagnetic wave. The Transmitter-chip used in this paper is made of gold (Au) in which two 10 μm-thick metal layers are spaced apart by 80 μm on a semi-insulating GaAs semiconductor substrate (SI-GaAs). A DC voltage of 80V is applied to the transmission line to form a strong magnetic field, and then an optical pulse of 14mW is applied to generate a THz electromagnetic wave. Figure 2-2(b) shows the receiver chip used to detect THz electromagnetic waves generated in transmitter chip. The chip is a dipole-type antenna grown on a GaAs semiconductor substrate grown at a low temperature (LT-GaAs). The shape of the dipole is a structure in which a metal of 10um thickness is separated by 200um intervals. An optical pulse of 14 mW is incident on the center of the dipole structure and THz electromagnetic wave is incident on the back of the receiver chip.

2.2 Long-Distance Measurement System

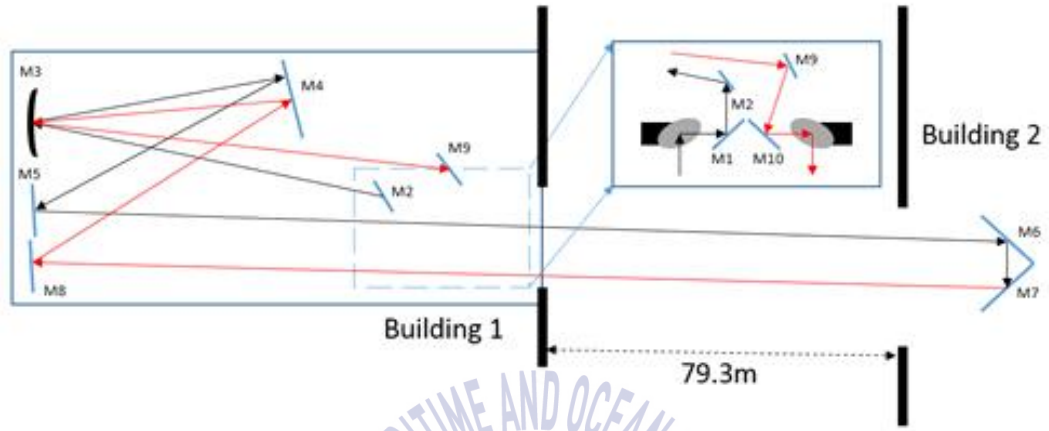

Figure 2-3 The measurement system for 186m transmission

The figure shows schematically the mirrors to installed to transfer generated THz electromagnetic wave to a long distance and the THz electromagnetic wave transmission path. In the figure, M represents mirror and the total transmission length is 186-m. M1 and M10 are installed between parabola mirrors and are designed to be removable by a magnet. M1 is used to propagate the generated THz electromagnetic waves over a long distance, and M10 is used to propagate the returned THz electromagnetic waves to Rx. The electromagnetic wave reflected by the Z-axis through the M1 mirror is reflected back on the M2 and transmitted to the M3. M3 is a spherical mirror that is used to reduce the spread of electromagnetic waves to Building 2, to transmit a long distance, and to collect the returning electromagnetic waves to maximize focusing on Rx. The focal length of the M3 was 125 inches (317.5 cm), located at a distance of 317.5 cm from M3 to Rx. All mirrors except M3 have an adjuster behind the mirror to fine-tune the angle. The M6 and M7 are located on the third floor of Building 2 (79.3m away). They are

manufactured at right angles so that incident THz electromagnetic waves can be reflected in parallel. It is also mounted on a 1.25 m support to match the height of the THz electromagnetic waves coming from building 1. In order to predict the path of the invisible THz electromagnetic wave, the path of the THz path and the helium-neon laser (He-Ne laser) between the parabolic mirrors were made equal. The helium-neon laser has a wavelength of 0.633 um in the visible region. Thus, the visible Helium-Neon laser can be used to control the path and then the THz electromagnetic wave measurement is performed.

A mirror for the 910m transmission of the THz electromagnetic wave is schematically shown in the figure 2-4(a). The difference from the 186m measurement is that M11 is placed in front of M6, M7, and THz pulse is sent to Building 3. In Building 3, M12 and M13 are installed at right angles as M6 and M7. It was also strongly fixed on the concrete to prevent the mirror from shaking in the wind. Building 3 with M12 and M13 and building 2 with M11 are separated by a straight line distance of 363m. Figure 2-4(b) shows that there is a sea in the path from building 2 to building 3. This path allows us to expect the influence of the sea. The total propagation distance of the THz pulse is 910 m and the distance influenced by the external environment is 883 m.

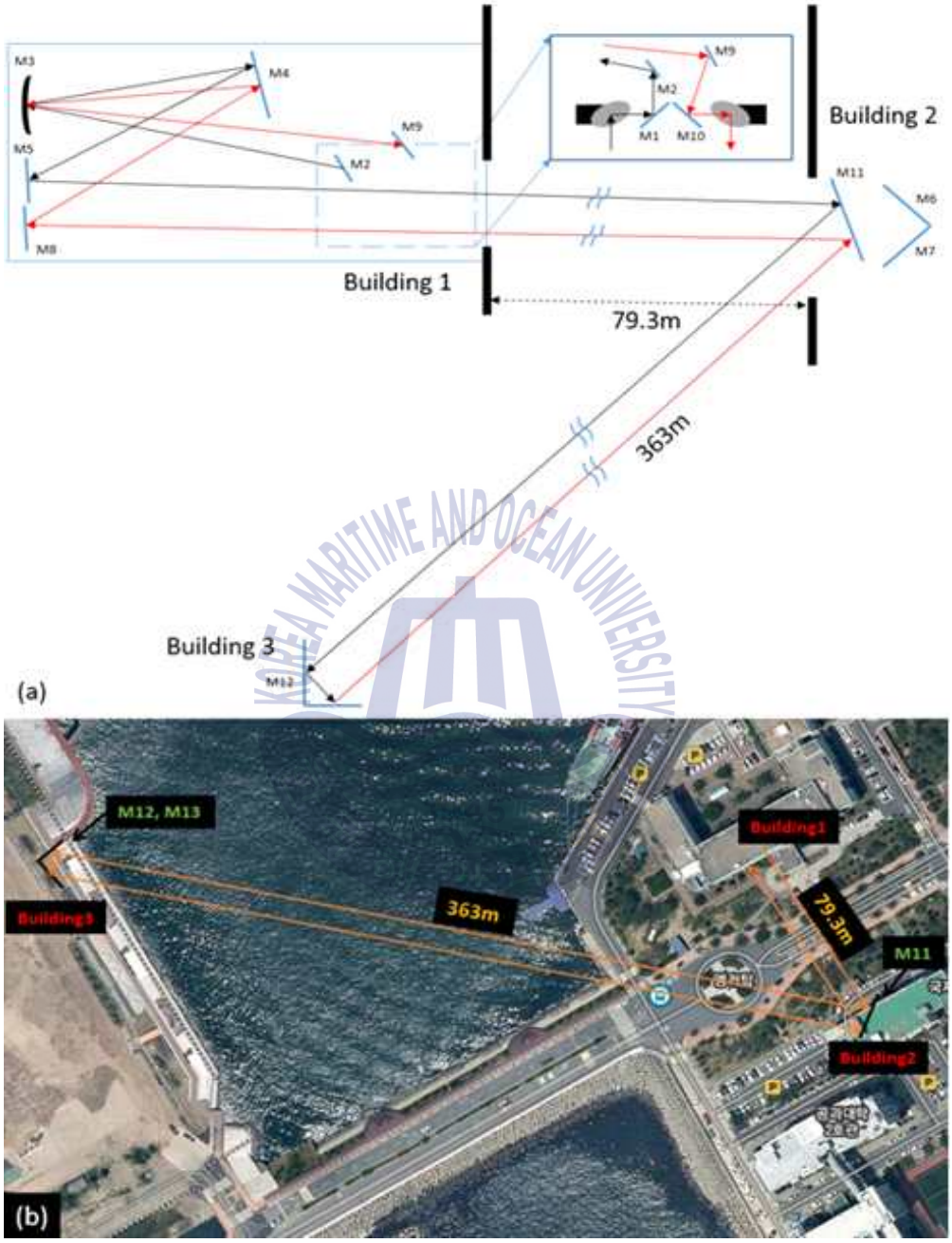

Figure 2-4 The measurement system for 910m transmission (a)Schematic representation of the path. (b) Photographic expression of path and surrounding environment.

Chapter 3. Long-Distance Measurement

3.1 Comparison of THz Pulses Over Distance

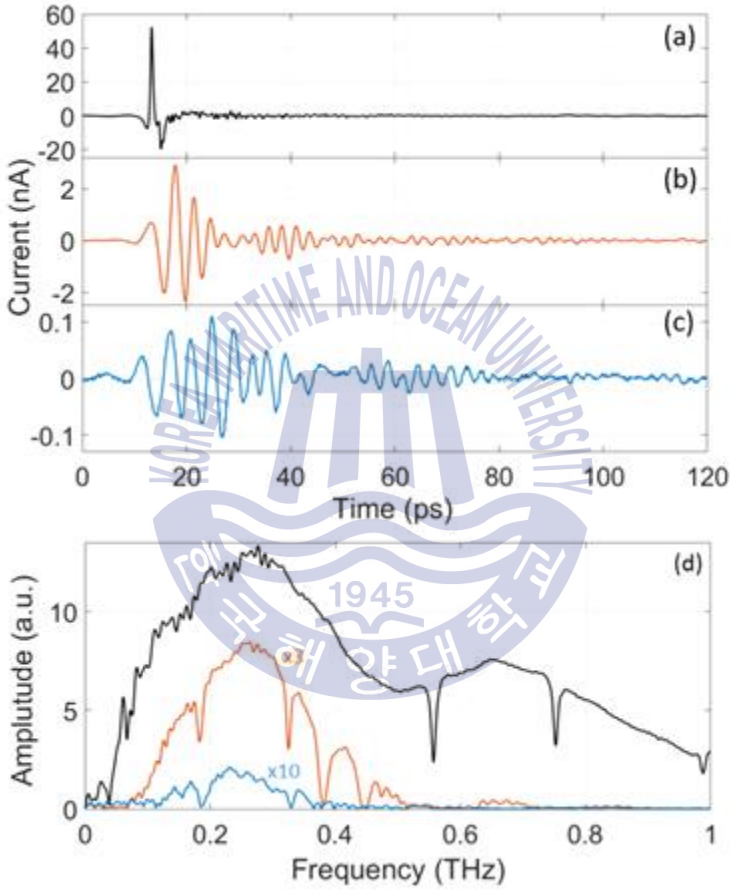

Figure 3-1 Measured THz pulse and spectrum (a)Reference. (b)186m. (c)910m. (d)corresponding spectrum.

The THz pulse measured according to the transmission distance is shown in the figure 3-1. The above three pulses were measured by moving the delay-line at intervals of 10 μm for a total of 2000 data. The optical laser

beam is moved by 20 μm while the delay-line is moved by 10 μm, and each measurement data is measured at g = 20×10^{-6}m / (3×10^{8} m/s) = 0.0667 ps intervals. Thus, the total measurement length is 133.4 ps and takes 380 seconds. Since the temperature and humidity continuously change during the measurement time of 380 seconds, the average value of the temperature and humidity recorded at intervals of 10 seconds was used and the WVD was obtained using the temperature and humidity. The instrument used for temperature and humidity measurements is the Testo 625, with a temperature resolution of 0.1 ℃ and a humidity resolution of 0.1 %.

Figure 3-1(a) shows the pulses measured at Rx through the parabolic mirrors where the THz pulse generated at Tx has no M1 and M10 mirrors. The total transmission length is 0.6m and the peak-to-peak is 71.98nA. In the laboratory, the temperature and humidity are kept constant at 22 ° C and 40 %, and WVD is 7.9 g/m3.

The pulse shown in Figure 3-1(b) is a pulse measured along the 186m path with M1 and M10 between the parabolic mirrors. The temperature and humidity of this pulse are 14.7 ° C, 71.25 % and WVD is 8.9 g/m3. The measured temperature and humidity are different from the actual temperature and humidity because the ground is 9.5 m below the path where the THz pulse travels to the ground between Building 1 and Building 2. The peak-to-peak is 5.26 nA, which is reduced to 7.3% of the reference pulse and the pulse shape is spread widely. This is because as the transmission length of the THz pulse becomes long, absorption by moisture becomes large.

Figure (c) shows a pulse taken after M11 and M11 are set up in front of M6 and M7 and then sent to M12 and M13 to increase the transmission distance. The total transmission length is 910m and the temperature and humidity at the time of measurement are 13.3 ° C and 73.7 % and WVD is 8.4g/m3. Also, because of the long distance, it was influenced by the external

environment and the size was reduced to 0.29% compared with the reference. Unlike the 186m measurement, because the distance was considerably longer, we also changed the location to measure temperature and humidity. The position was measured next to M13 and at the bus stop shown in the figure 2-4(b). The WVD was obtained by measuring the temperature and humidity at each position, and the median value of WVD was selected. The WVD was obtained from the measured temperature and humidity at each position, and the median value of the obtained WVD was selected.

The spectra of Figures (a), (b) and (c) are shown in Figure (d). Compared with the reference spectrum, the spectra of 186m and 910m pulses are significantly reduced in amplitude due to high absorption by moisture. Therefore, for comparison, the spectra of 186m and 910m were multiplied by 3 and 10 times, respectively. 186m, and 910m spectra were all absorbed at above 0.5 THz and could not be detected. In the reference spectrum, the resonance is not observed near 0.183, 0.325, and 0.380 THz due to the low influence of moisture. However, the resonance appears in the spectrum of 186m and 910m, which is affected by moisture by moving a long distance. The 910m resonance has maximum absorption and touches the bottom, but the energy of 186m resonance remains.

3.2 Pulse Matching

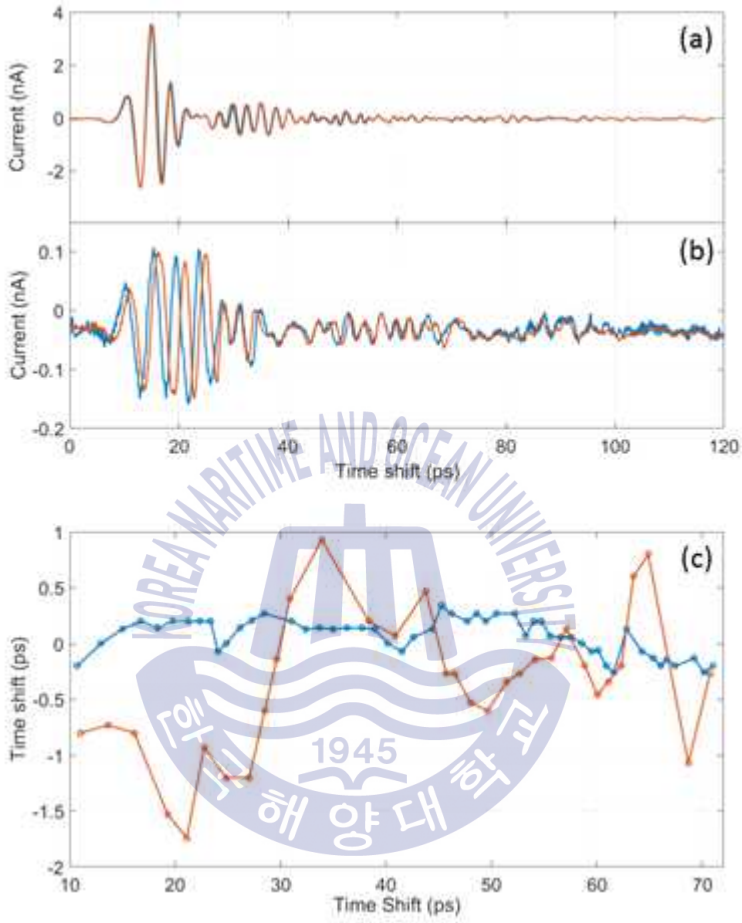

Figure 3-2 Overlapping two consecutive pulses (a) 186m measurement. (b)910m measurement. (c)Time variation of each peak. The blue solid line is the peak difference of 186 m pulses. The orange line is the peak difference of 910 m pulses.

Long path THz pulse measurements are mostly propagated outdoors, not indoors. Since the temperature and humidity change instantaneously, a time shift or an amplitude difference occurs between two measured pulses even

after continuous measurement. The following figure shows the 186m pulse and the 910m pulse continuously measured, and the table shows the measurement time, temperature, relative humidity and WVD of the waveform. Each measurement took about 6 minutes and 30 seconds, and M11 was installed after 186 meters of measurement. Two pulses of 910 m were measured thereafter.

Figure 3-2(a) shows the overlap of two pulses in order to see the continuity of 186 m pulses measured continuously. The peak-to-peak of each pulse is 6.15 and 6.23 nA, which is 1.3% different. It is somewhat misaligned at around 30ps, but it is generally a good match. Two pulses of 910 m continuously measured are shown in the figure3-2(b). The peak-to-peak of each pulse is 0.26 and 0.24 nA, which is 8.3% different. It can be seen that the two pulses do not fit well throughout the measurement, despite two successive pulses.

Distance (m)	*Measurement Start Time*	*Temperature (℃)*	*Relative Humidity (%)*	*WVD*
186	16:57	13.9	52.5	6.25
186	17:05	13.2	53.5	6.09
910	17:23	12.7	58.2	6.41
910	17:30	12.4	58.9	6.36

Table 1 The external environment when the pulse in Figure 3-2 is measured

As shown in the table3-1, the 186m measurement shows that the WVD change between the first pulse and the second pulse is 0.16 g/m3, while the WVD change of the 910m measurement is less than the 186m measurement with 0.05 g/m3. Nonetheless, the successive measurements of the 910m two pulses do not match well. It can be interpreted that the 910m measurement is more affected by moisture because the measurement distance is 4.89 times

longer than the 186m measurement. For other reasons, as shown in the figure2-4, THz electromagnetic waves propagate 434 meters above sea level. Therefore, the air above the sea, which has a relatively large amount of moisture, can affect the traveling THz electromagnetic waves.

Figure 3-2(c) shows the difference at each peak point in figures 3-2(a) and (b). The blue graph shows the difference of each peak in the 186m measurement, and the orange graph shows the difference of each peak in the 910m measurement. The change in the 186m peak is less than the change in the 910m peak, with the standard deviation of 186m being 0.16 and 910m being 0.63.

Chapter 4. THz Pulse Characteristics Varying by WVD

4.1 THz pulse propagated 186m according to WVD

THz electromagnetic waves have high water absorption rate, so THz pulses are measured when WVD is different as follows to investigate how atmospheric water vapor affects THz pulse. Each pulse was measured after measurement of the reference and the other days measurements were made because we can't control the external environment. The measured data for each pulse is a total of 2000 data in a 10-μm step, and the total length is 133.2 ps.

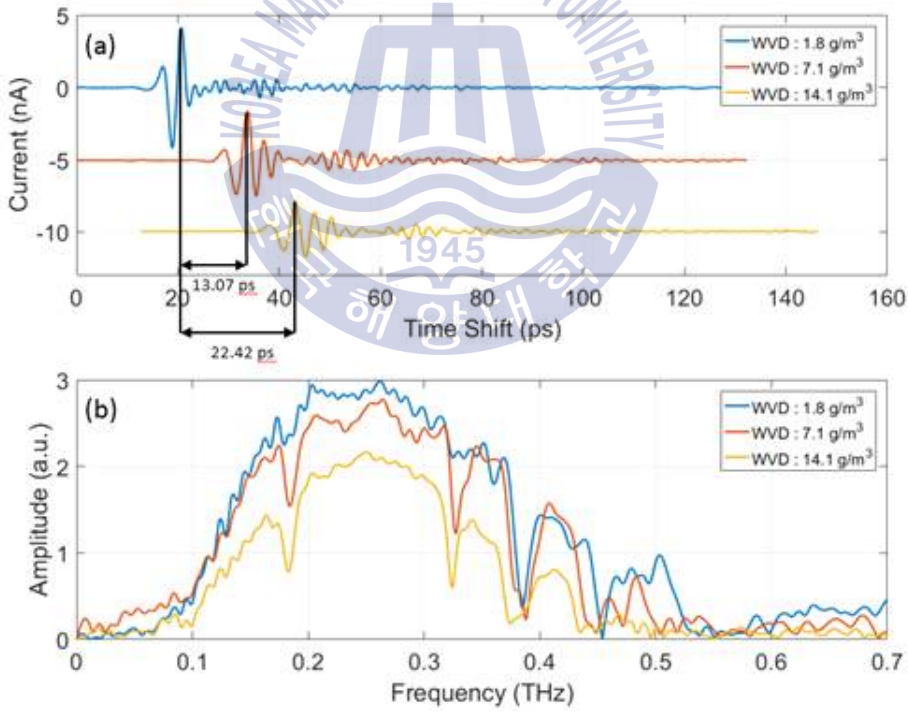

Figure 4-1 (a)186 m measurement change according to WVD. (b)The spectrum corresponding to (a)

The THz pulse measured according to WVD can be seen in Figure 4-1(a). Since the position of the THz pulse varies depending on the atmospheric condition, the measurement was performed by adjusting the start position of the delay-line scan. Therefore, the yellow waveform starts measuring behind the other two waveforms, but the total length scanned is the same. Blue pulses were measured on very dry days with a WVD of 1.8 g/m3. And the peak-to-peak is 8.4 nA. The WVD of the orange and yellow pulses is 7.1 and 14.1 g/m3, respectively, and the peak-to-peak is 5.9 and 3.8 nA, respectively. Because of the increased amount of water vapor in the atmosphere, much absorption occurs, a time delay occurs between the pulses, and the shape of the pulses becomes wider. The THz pulse traveling at the same distance can be interpreted as the increase of the atmospheric refractive index because of the higher delay in the case of higher water vapor density.

Figure 4-1(b) shows the spectrum of the THz pulse measured in figure 4-1(a). At more than 0.5 THz, spectral energy can be observed at 0.1 ~ 0.5 THz, which is relatively low frequency band, because it is absorbed by moisture. As the WVD increases, the amplitude and bandwidth of the spectrum decreases, which is similar to the result of previous studies [9,17,18]. In the blue spectrum with a small amount of water vapor, there is no resonance caused by moisture at 0.183 and 0.325 THz. However, the orange and yellow spectra show resonance due to moisture. The position of the resonance that occurs here differs from the orange spectrum to the yellow spectrum because of the low signal-to-noise and pulse jitter.

The figure 4-2 shows the peak points of all 186 m pulses measured according to WVD. The black dot and the solid line represent the peak point of the actual measured pulse and the fitting line, respectively. However, this value is a value that can be changed, not a fixed value, since the reference pulse is determined according to the position at which the measurement

starts. Therefore, the starting point can be translated to 0, as shown by the circle and dotted lines. The slope of the fitting line is 1.58, which means that the THz pulse is delayed by 1.58 ps when WVD is increased by 1, and the standard deviation is 2.92.

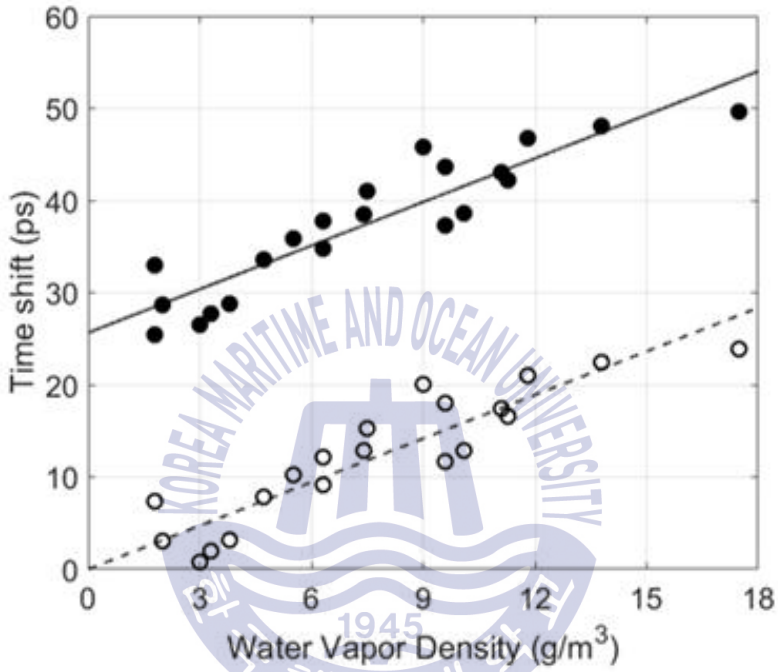

Figure 4-2 The Time-shift of the measured 186m pulses

There are some errors in determining the delay from the time domain to the peak of the pulse. The first is that the external situation continues to change during the measurement. The time it takes to acquire one pulse is about 6 minutes and 30 seconds. During this time, the external temperature and humidity continuously change. The second is that the shape of the pulse changes as the WVD changes, as shown in the figure 4-1. Therefore, we applied the technique of confirming the phase shift in the frequency domain rather than checking the time-delay in the time domain.

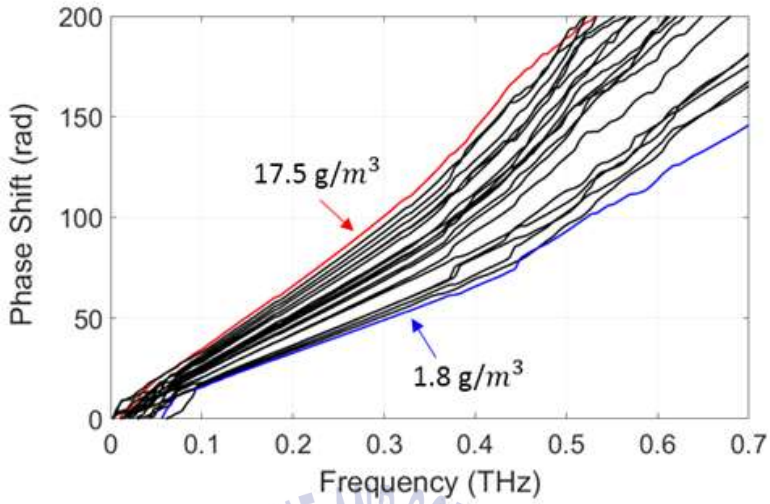

Figure 4-3 The phase-shift of the measured 186m pulses

The figure 4-3 shows the measured 186m pulse as the phase value in the frequency domain. Due to the presence of spectral energy, the phase-shift is increasing linearly within the range of 0.1 to 0.4 THz. On the other hand, phase-shift is cluttered above 0.4 THz, which is absorbed by moisture and has little spectral energy. In addition, the phase shift shifts slightly around 0.183 and 0.325 THz with moisture resonance. In addition, the phase shift is slightly shifted in the vicinity of moisture resonance. The blue line in the figure 4-3 is when the WVD is the lowest of 1.8 g/m3. On the other hand, the data when WVD is the highest 17.5 g/m3 is red. When we look at the value at 0.25 THz, the blue line is 41.1 radian, the red is 83.43 radian, and the red line is shifted by 42.33 radian when it is 0.25 THz than the blue line. If we change this phase-shift to a time-shift value by the following simple formula, we get $\triangle t = \frac{\Phi}{2\Pi f} = \frac{42.33}{2\Pi * 0.25\,THz} = 27.5\,ps$. This value is similar to the difference between the time-shift at the lowest WVD and the time-shift at the highest in Figure 4-2.

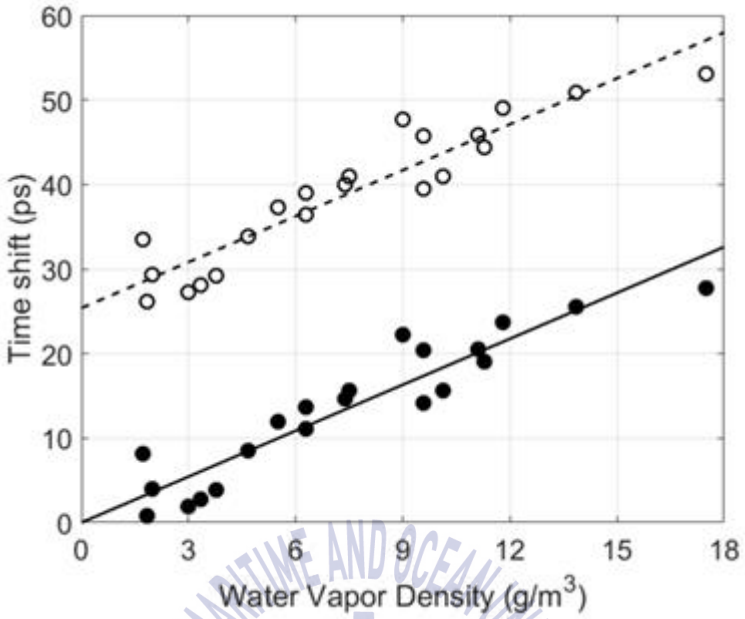

Figure 4-4 Time-shift according to WVD by phase-shift of measured 186m pulse

Applying the value obtained by converting the phase-shift to time-shift in this way, all the data shows a graph with data and slope as shown in the figure 4-4. Circle is the time-shift converted value of 0.25THz of the phase-shift data, and the dotted line is the fitting line. Since it depends on the phase-shift value of the reference pulse, it can be moved in parallel to the graph shown by the dotted line and the solid line.

The figure 4-5 shows a time shift graph obtained by time-delay and a time shift graph obtained by phase shift. The standard deviation of the phase-shift measurement is 2.85, which is lower than the time-delay measurement, so the data is close to the fitting line. Thus, it can be seen that the data of the phase-shift measurement is less scattered. The slope of the fitting line was 1.81 and measured 1.14 times higher than the slope of the time-shift obtained by the time-delay.

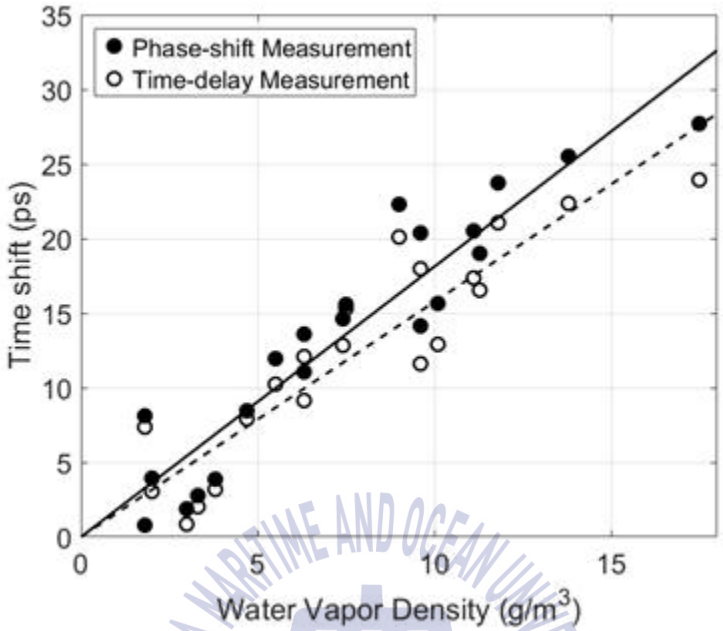

Figure 4-5 Time-shift according to WVD by Phase-shift of measured 186m pulse and Time-delay of measured 186m pulse

As shown in the figure4-1(b), when the WVD increases, the depth of resonance increases at 0.183 and 0.325 THz, and the transmittance as shown in the figure 4-6 (a) can be obtained. Since the WVD is not constant during the measurement, the absorption line is not constant and there is some variation. The blue graph is obtained when WVD is 1.8 g/m3 and the red graph is the transmittance obtained when WVD is 17.5 g/m3. The black graph shows that the transmittance decreases as the WVD increases, and the transmission coefficient according to WVD is shown in the figure 4-6(b). The transmission coefficient of 0.325 THz is lower than that of 0.183 THz because the absorption by moisture increases as the frequency increases [16]. However, since the THz beam power is greater at 0.325 THz, the absorption line is better.

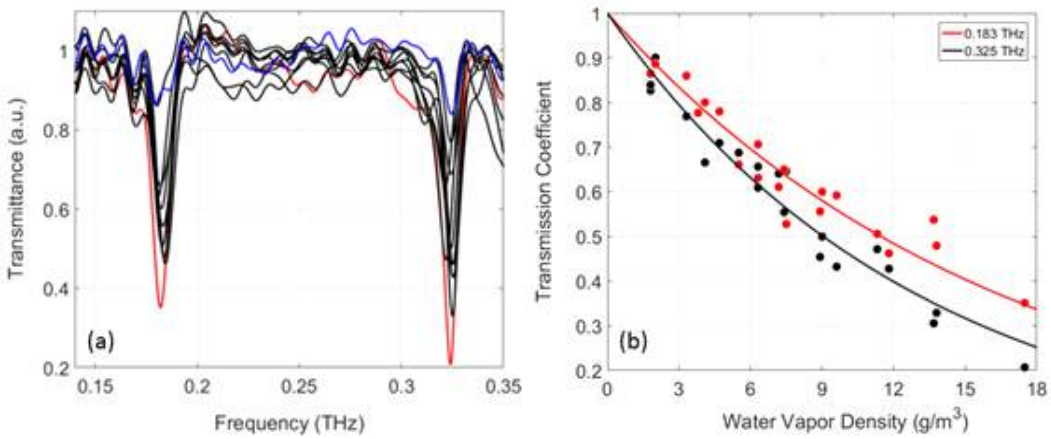

Figure 4-6 (a)Transmittance 186m measurement with different WVD. (b) Transmission coefficient at 0.183 and 0.325 THz absoption lines.

4.2 THz pulse propagated 910m according to WVD

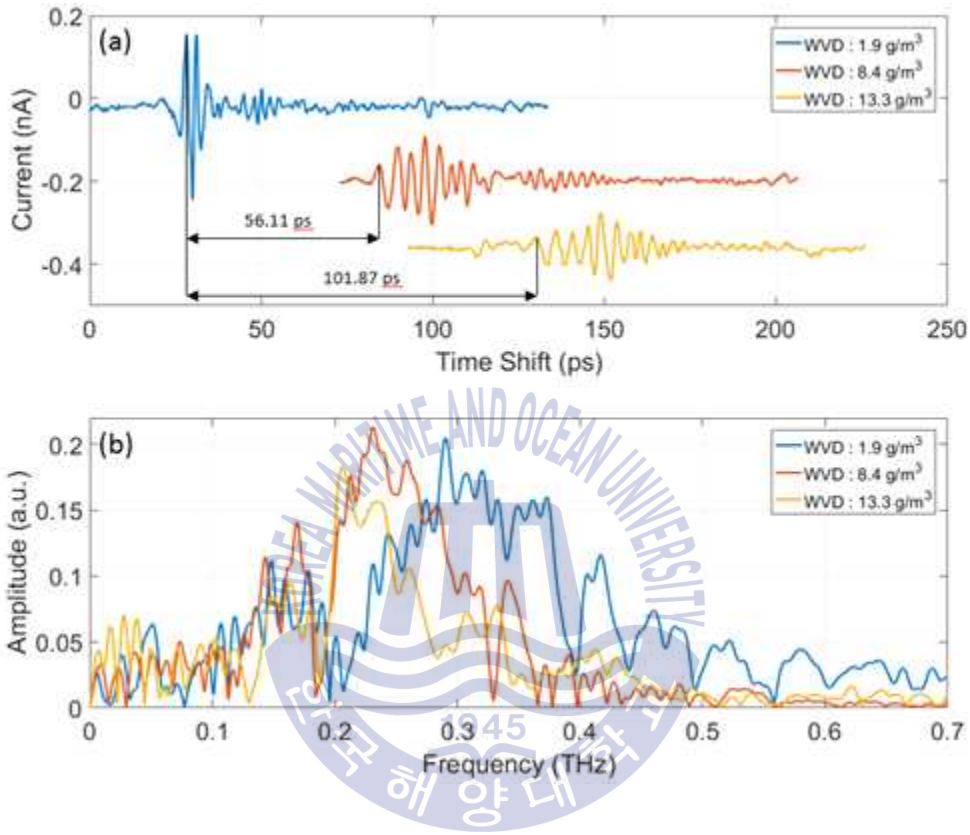

Figure 4-7 (a)910 m measurement change according to WVD. (b)The spectrum corresponding to (a)

The 910m THz pulse measured according to WVD is shown in Figure (a). As with the 186m measurement, it can be seen that as the WVD increases, the delay of the pulse occurs but the delay is greater. The blue and orange pulses of 186m pulses were delayed by 13.07 ps while the 910m blue pulses and orange pulses were delayed by 56.11 ps. The yellow 910m pulse has a much higher pulse delay than the yellow 186m pulse even though the WVD is lower. Therefore, since the distance increased from 186m to 910m rather than

the effect of WVD, the effect of external moisture was more affected and the pulse was delayed more. Another feature is that the 910m pulse is smaller than the 186m pulse and the shape spreads widely.

The blue pulse has a peak-to-peak greater than other orange or yellow pulses and a pulse width of about 20 ps. However, the large orange and yellow pulses of WVD are smaller than the blue pulses in magnitude, and the width of the pulse spreads more than 40ps due to the influence of group velocity dispersion by moisture. However, since the orange and yellow pulses are WVD larger than the blue pulses, it can be seen that the size of the pulse is smaller than that of the pulse and that the width of the pulse spreads more than 40 ps due to the influence of the group velocity dispersion by moisture.

Figure 4-7(b) is a graph showing the frequency domain by (a) pulse FFT. Most of the energy is absorbed while transmitting 910m, and the S / N is poor, so there is a lot of noise in the spectrum, but there is energy remaining between 0.1 and 0.4THz. Since the blue spectrum with WVD of 1.9 g/m3 is less absorbed by moisture, spectral energy is visible above 0.4 THz, whereas the orange and yellow spectrum with higher WVD shows a decrease in bandwidth. However, since there is still energy in the range of 0.1 ~ 0.2 THz and 0.2 ~ 0.3 THz, THz long-range wireless communication is possible.

The figure 4-8 shows the time shift of measured 910m pulse according to WVD in the time domain. The red circle represents the first pulse point of each data, the dotted line is the fitting line of the data, and the slope is 10.19. Like 186m, since the time shift value changes according to the position of the reference pulse, it is shifted to 0 in parallel. The inside of the laboratory, 27m, has little influence on the actual measurement because the temperature and humidity are kept constant. Therefore, the distances affected by the external environment in the 186 and 910m measurements are 159m

and 883m, respectively. The 910m measurement was influenced by the external environment 883m / 186m = 5.55 times more than the 186m measurement. Thus the 910m time-shift slope should be 5.55 times the 186m time-shift slope but higher than that. The cause of this error could be found in the temperature and humidity measurement location and path difference. Although both temperature and humidity measurements were made on the ground, the 910m measurement travels over the ocean, unlike the 186m measurement, which travels between the building and the building, so the measured temperature and humidity are clearly different from the actual path temperature and humidity. Therefore, time-delay occurred more than calculation. Accurate WVD measurement techniques are required to reduce this error.

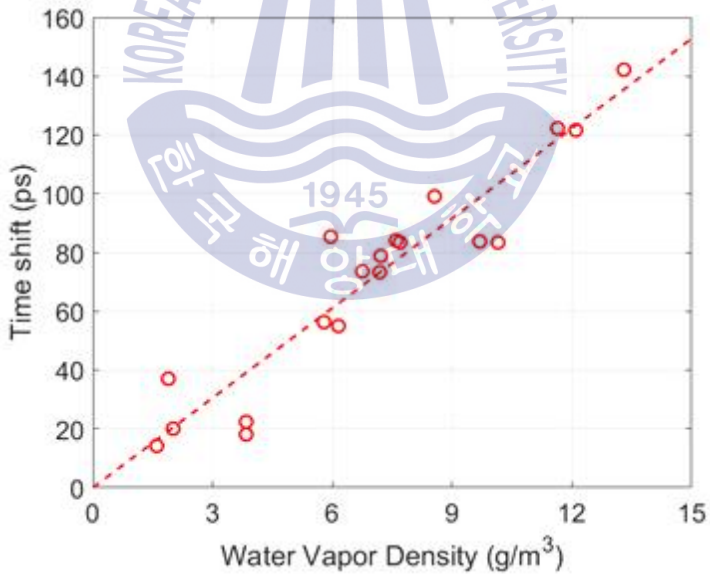

Figure 4-8 The time-shift of the measured 910m pulses

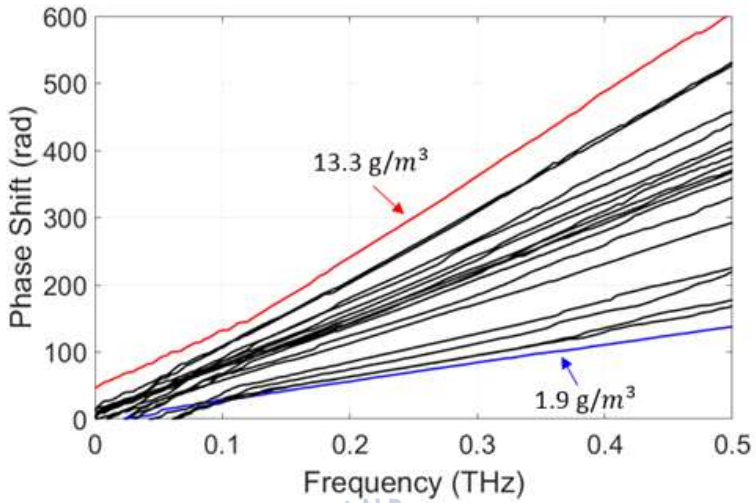

Figure 4-9 The phase-shift of the measured 910m pulses

Like the 186m measurement, the phase-shift of measured 910 pulses is also shown in the figure 4-9. The blue line is when the WVD is the lowest at 1.9 g/m3, the red line is the highest WVD at 13.3 g/m3, and the black lines are the phase-shift graph by WVD. As can be seen in the figure, the 910 m measurement shows that the lines are not linearly, because the spectral energy is small. It increases linearly in the range between 0.2 and 0.3 THz, where relatively spectral energy remains.

Figure 4-10 shows the result of converting the phase shift value into the time-shift value and classifying it according to WVD. dot represents the time shift of the phase shift value of each data according to WVD at 0.25 THz, and the solid line represents the fitting line.

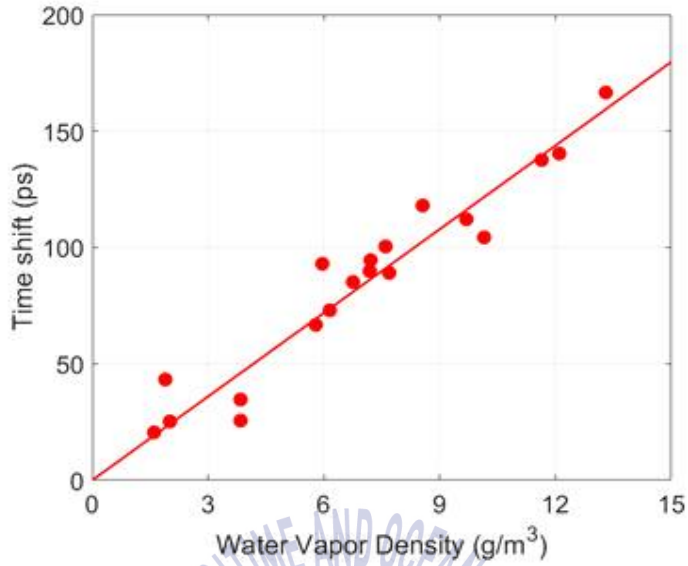

Figure 4-10 Time-shift according to WVD by phase-shift of measured 910m pulse

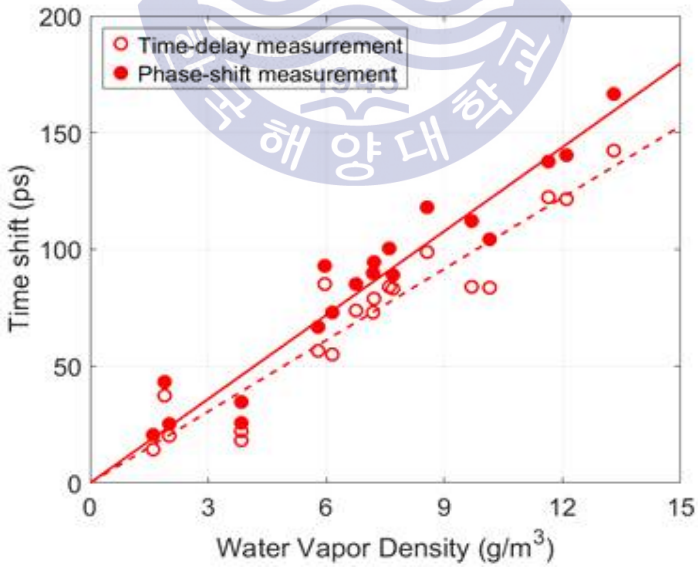

Figure 4-11 Time-shift according to WVD by Phase-shift of measured 910m pulse and Time-delay of measured 910m pulse

The figure 4-11 shows a time-delay measurement and a phase-shift measurement. The standard deviations of the time-delay measurement and the phase-shift measurement are 12.17 and 11.13, respectively, and the phase-shift is well distributed in the fitting line. Therefore, it can be concluded that the data of the phase-shift measurement is less scattered and the accuracy is higher. The slope of the fitting line was 10.19 and 11.98, respectively, and the phase-shift measurement was higher.

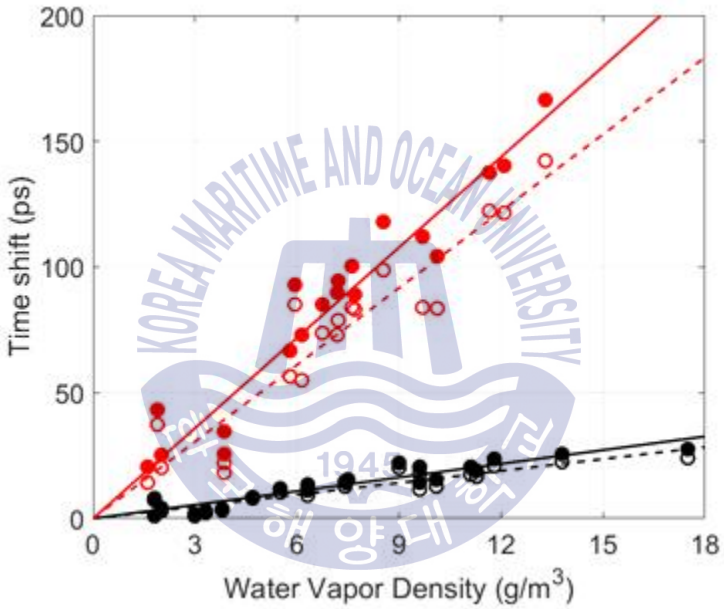

Figure 4-12 Figure 4-5 and Figure 4-11 on the same axis.

The figure 4-12 shows the figure 4-5 and the figure 4-11 drawn in the same axis for comparison. All the images in black are 186m measurement and all red is 910m measurement. Circle is time shift value obtained by time-delay measurement. Dot is time shift value obtained by phase shift measurement. It can be seen that the 910m measurement data shows a lot of time shift depending on the WVD. The slope ratios of the time-delay measurement and the phase-shift measurement of 186m and 910m are 1.15 and 1.18,

respectively.

Chapter 5. Comparison of Theory and Measurement

In the previous research and experiments in this paper, we could confirm the time shift by the time delay and phase shift of the THz pulse according to the WVD change. This time delay and phase shift may be said to be the change in the refractive index of the path through which the THz pulse propagates. As shown in the figure 5-1, 13.5m is the distance of the THz pulse in the laboratory, and 159m and 883m is the distance propagated from outside the laboratory. Since the temperature and humidity are kept constant in the laboratory (22 ° C, 40 %), there is little change in the environment in every measurement. However, the environment outside the laboratory is continuously influenced by the weather and the season of the measurement period.

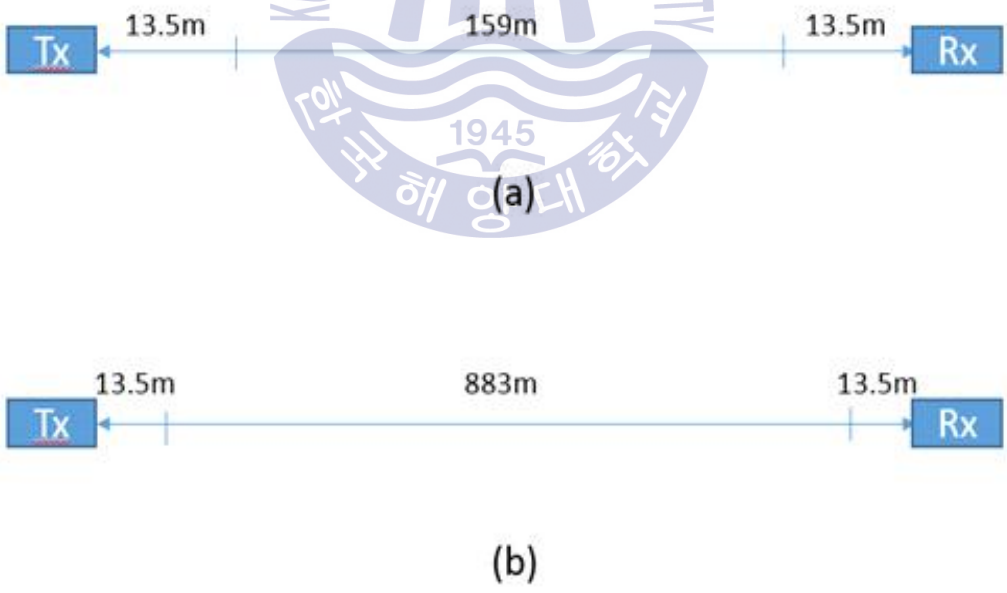

Figure 5-1 (a) Schematic representation of 186m measurement. (b) Schematic representation of 910m measurement

In other words, the refractive index of the air inside the laboratory remains constant for each measurement, while the refractive index of the air outside the laboratory varies from one measurement to the next. Therefore, the speed of the THz electromagnetic wave changes according to the refractive index of the air outside the laboratory, so that the time delay and the phase shift can be said to have occurred. In this chapter, theoretically calculating how much the THz pulse moves according to the WVD and comparing with the actual measurement is shown.

5.1 Calculation of refractive index of the atmosphere

The refractive index of the atmosphere (n-1) can be expressed by the following three terms.

$$(n-1)10^6 = K_1\frac{P_d}{T} + K_2\frac{e}{T} + K_3\frac{e}{T^2} \quad (1)$$

The first and second terms are charge distortion due to dry air and water vapor, respectively. The third term is the directional effect of the electric dipole of water vapor, which is influenced by the field. Pd is the dry air, e is the pressure of water vapor (hPa), and T is the absolute temperature (K). $K1$, $K2$, and $K3$ are constant values for each term, and in the 1950s there was a lot of research to find these values [19,21]. In this paper, we have calculated the atmospheric refractive index using Smith & Weintraub's K value, which is still being investigated [19]. Therefore, the above equation can be expressed as follows.

$$(n-1)10^6 = 77.6\frac{P_d}{T} + 72\frac{e}{T} + 3.75\times10^5\frac{e}{T^2} \quad (2)$$

The atmospheric pressure was P = Pd + e and the atmospheric pressure in Busan, where this study was conducted, was obtained from the data of the Korea Meteorological Administration according to date and time. e can be obtained from the measured temperature and humidity [20]. In addition, Pd can be calculated from P obtained from Korea Meteorological Administration and the temperature and humidity measured. The above equation is calculated by replacing WVD with hPa using hPa units.

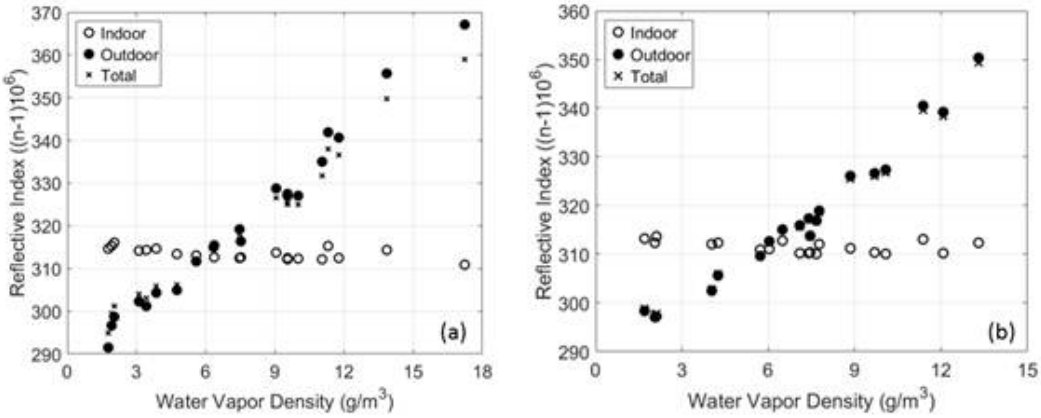

Figure 5-2 (a) refractive index of measured 186m data. (b) refractive index of measured 910m data.

(A) and (b) show the refractive indices obtained by putting the measurement data of 186m and 910m into equation (2), respectively. "Indoor" is the refractive index due to the internal environment of the laboratory. As the WVD increases, the refractive index decreases slightly. This is because the temperature and water vapor pressure are constant in equation (2), but the refractive index of dry air depends on atmospheric pressure. This is because the temperature and water vapor pressure are constant in equation (2) while the refractive index of dry air depends on atmospheric pressure. The extent of change is not large. "Outdoor" is the refractive index due to the external environment of the laboratory, and the value of refractive index changes significantly with increasing WVD. As a result, it can be seen that the external environment greatly affects the refractive index of the atmosphere. "Total" in figure 5-2(a) is "Indoor" X 27m/186m + "Outdoor" X 159m/186m. Besides, "Total" in figure 5-2(b) is "Indoor" X 27m/910m + "Outdoor" X 883m/910m. It can be seen that the difference in the external environment is slightly reduced due to the constant internal state of the laboratory.

5.2 Time-shift Calculation and Comparison with Measurement

When each pulse is measured by the above equation (2), the refractive index can be calculated by putting the recorded temperature, WVD and atmospheric pressure, and the time-shift (Δt) can be calculated using this refractive index. The time-shift can be obtained by , where L is the distance (186m, 910m) at which the THz pulse is propagated and c is the speed of light.

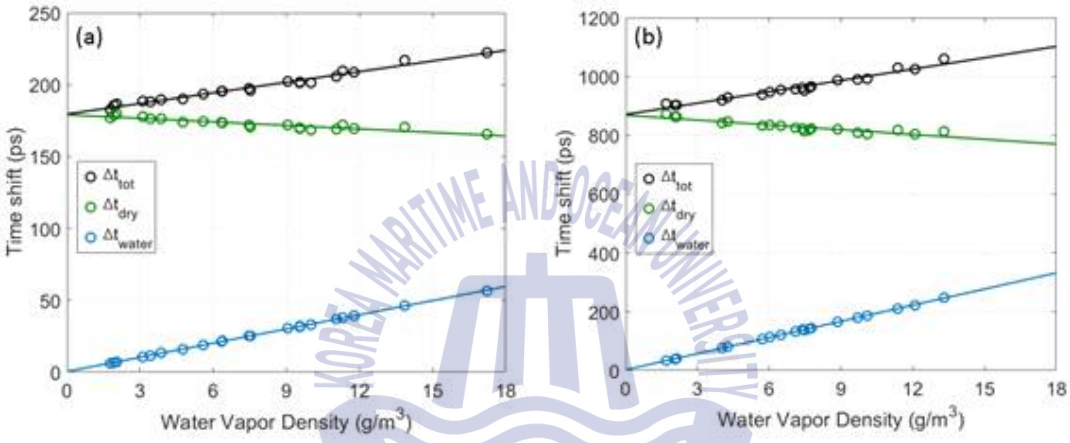

Figure 5-3 (a)Calculated Time-shift by measured 186m data (b) Calculated Time-shift by measured 910m data

The time-shift is calculated by the refractive index of 186m "Total" obtained above, and according to WVD, a graph such as Δt of figure 5-3(a). Circle is the calculated value, and the solid line represents the fitting line. Even if WVD is 0, there is a time-shift because there is a refractive index due to dry. However, for the graph of the time shift due to the water vapor outside the laboratory, the time shift due to dry air and the time shift due to the indoor environment must be subtracted from the total time shift. The time-shift due to the refractive index of the outdoor air and indoor air is shown in Δtdry. Time-shift due to external water vapor is obtained by subtracting Δttot from Δtdry. Δtwater is time-shift due to pure external

water vapor, and the degree of time-shift can be known as WVD increases. Similarly, when the calculated time-shift is obtained with a refractive index of 910 m, the graph of figure 5-3(b). The refractive indices obtained are similar in figure 5-2(a) and (b) to each other, but differ greatly in the time shift due to the different propagation distances of THz pulses. The slopes of 186m and 910m Δtwater are 3.3 and 18.3, respectively.

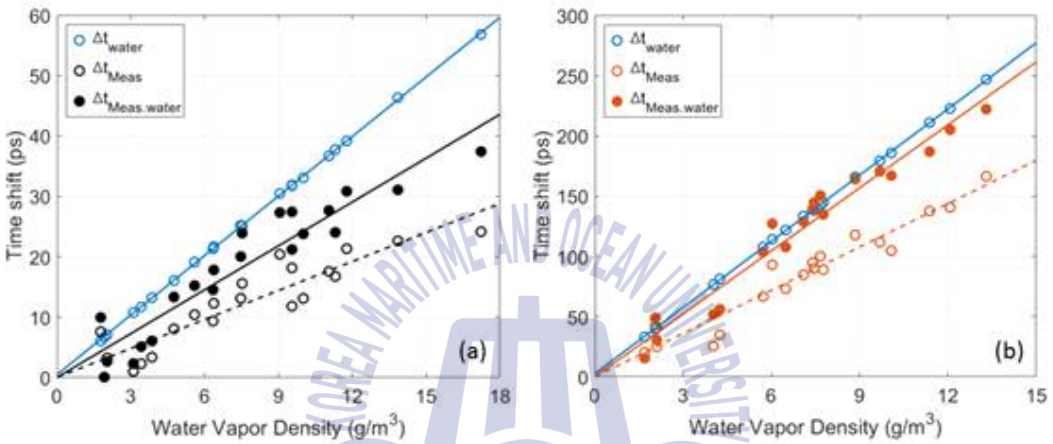

Figure5-4 (a)Measured 186m time-shift and calculated 186m time-shift. (b)Measured 910m time-shift and calculated 910m time-shift.

Figures (a) and (b) show the measured 186m and 910m data and the calculated time-shift. The time-shift due to external water vapor was calculated by calculating the refractive index of air from equation (2). In actual measurement, however, the time-shift due to the atmospheric dry air component and the water vapor can't be divided. Therefore, $\Delta tMeas$ includes not only the time-shift due to external water vapor but also the components of the inside air and the outside air. Therefore, as shown in the figure 5-4 (a) and (b), there is a large difference between $\Delta twater$ and actual measured data Δtwater. In order to see the experimental data and calculated values accurately, the time-shift value of the inside air and outside air calculated for the experimental data was subtracted and expressed as $\Delta tMeas.water$ in the figure 5-4(a) and (b). The slope of $\Delta tMeas.water$ at 186m

and 910m is 2.4 and 17.4, respectively, which is smaller than the slope of Δ *twater*. The first difference is that the actual transmitted THz pulse propagates above 10 m above ground and the temperature and humidity are measured at ground level, which is the WVD calculation error due to this difference. The second is that the parts supporting the mirror may experience slight path differences due to temperature.

Chapter 6. Conclusion

THz-TDS was used to measure THz pulses through a 910m distance, and the THz electromagnetic waves varying with distance were analyzed. As the distance increases, the absorption by moisture increases, so that the size of the measured THz pulse decreases. In addition, since the energy of the spectrum decreases in the frequency region confirmed by the FFT and the absorption becomes higher toward the high frequency, it is confirmed that the energy exceeding 0.5 THz is absorbed and disappears. Furthermore, moisture resonance was also observed at 0.183 and 0.325 THz, which did not appear at short distances.

In the 186m and 910m measurements, it was observed that as the WVD increases, the size of the THz pulse measured decreases and the shape broadens. The decrease in the size of the THz pulse is due to the increase in absorption by moisture, and the spread of the pulse shape is influenced by the diffusion of the group velocity. In addition, the spectral size and band-width decrease in the frequency domain. In particular, as the WVD increases, the resonance at 0.183 and 0.325 THz deepens in the 186m measurement. We can see that the depth of resonance is deeper at 0.325 THz than 0.183 THz, which is presumably because the higher the frequency, the more absorption by moisture.

Obtaining the THz pulse with a time delay in the time domain may not be accurate due to changes in the measurement environment during the measurement. Therefore, we compared the time shift obtained by the phase shift and the time shift obtained by time delay. The data obtained by the phase delay showed a small standard deviation for both the 186m and 910m measurements, but the data obtained by the time delays fit better in the 186m and 910m tilt calculations.

In the Smith & Weintraub study of atmospheric refraction, we calculated the atmospheric refractive index when measuring long-range THz pulses. We compared the time shift calculated using this index to the time shift of the measured pulse. Since the long-distance THz transmission has a complex environmental change compared with the previous studies, only time-shift due to air moisture is calculated. There is a difference between the slope of Δtwater and the slope of $\Delta tMeas.water$, which can be interpreted as the error of the WVD measurement and the parts supporting the mirror expand and contract as the temperature changes.

Finally, long-range THz studies based on WVD are likely to be used in applications such as THz communications in the atmosphere and hazardous gas monitoring.

Reference

[1] R.H. Jacobsen, D.M. Mittleman, and M.C. Nuss, "Chemical Recognition of Gases and Gas Mixtures with Terahertz Waces," opt. lett., Vol.21, p.2011 (1996).

[2] C. Ludwig. et al., "Electrodynamic c-Axis Properties of YBa2Cu307-thin films in the Thz Frequency Regime," Physica Stat. Solidi B. Basic Research, Vol.213, p.405 (1999)

[3] B.B. Hu and M.C. Nuss, "Imaging with terahertz waves," Opt. Lett., Vol.20, p.1716 (1995)

[4] R.M. Woodward. et al,. "Terahertz Pulsed Imaging of Skin Cancer in the Time and Frequency Domain," J. Biol. Phys., vol. 29, pp. 257-261 (2003).

[5] M.R. Leahy-Hoppa et al., "wideband terahertz spectroscopy of explosives," Chem. Phys. Lett., vol. 434, no. 4-6, pp. 227-230 (2007).

[6] Y.C. Shen et al., "Detection and identification of explosives using terahertz pulsed spectroscopic imaging," Appl. Phys. Lett., vol. 86, no. 24, p. 241 116 (1986).

[7] Walker, C. K., 2015. *Terahertz Astronomy*. CRC press.

[8] Foltynowicz, R. J., Wanke, M. C., and Mangan, M. A., 2005. Atmospheric Propagation of THz Radiation. Sandia National Lab. Sandia Rep. SAND2005-6389.

[9] Yang, Y., Shutler, A., & Grischkowsky, D., 2011. Measurement of the transmission of the atmosphere from 0.2 to 2 Thz. Optics express, 19(9), 8830-8838.

[10] Melinger, J, S., Yang, Y., Mandehgar, M., & Grischkowsky, D., 2012. Thz detection of small molecule vapors in the atmospheric transmission windows.

Optics express, 20(6), 6788-6807.

[11] Yang, Y., Mandehgar, M., & Grischkowsky, D., 2012. Time domain measurement of the Thz refractivity of water vapor. Optics express, 20(24), 26208-26218.

[12] Yang, Y., Mandehgar, M., & Grischkowsky, D., 2012. Understanding THz pulse propagation in the atmosphere. Terahertz Science and Technology, IEEE Transactions on, 2(4), 406-415.

[13] Liebe, H. J., 1983. An atmospheric millimeter wave propagation model (No. NTIA-83-137). NATIONAL TELECOMMUNICATION AND INFORMATION ADMINISTRATION BOULDER CO INST FOR TELECOMMUNICATION SCIENCES.

[14] Yang, Y., Mandehgar, M., & Grischkowsky, D., 2014. Determination of the water vapor continuum absorption by THz-TDS and Molecular Response Theory. Optics express, 22(4),. 4388-4403.

[15] Yao, J., Wang, R., Cui, H., & Wang, J., 2012. Atmospheric Propagation of Terahertz Radiation. REMOTE SENSING-ADVANCED TECHNIQUES AND PLATFORMS, 371.

[16] Slocum, D. M., Slingerland, E. J., Giles, R. H., & Goyette, T. M., 2013, Atmospheric absorption of terahertz radiation and water vapor continuum effects. Journal of Quantitative Spectroscopy and Radiative Transfer, 127, 49-63.

[17] Moon, E. B., Jeon, T-. I., & Grischkowsky, D., 2015. Long-Path THz-TDS Atmospheric Measurements between Buildings. IEEE Trans. Terahertz Sci. Technol. 5(5), 742-750.

[18] Kim, G. R., Jeon, T-. I., & Grischkowsky, D., 2017. 910-m propagation of THz ps pulses through the Atmosphere. Optics express, 25(21),. 25422-25434.

[19] Smith, Jr E, K., Weintraub, S., 1953. The Constants in the Equation for Atmospheric Refractive Index at Radio Frequencies. Proc. IRE, 41, 1035-1037

[20] International Telecommunication Union. 2016. The Radio Refractive Index: Its Formula and Refractivity Data. Recommendation ITU-R P.453-12.

[21] Essen, L. & Froome, K. D., 1951. The Refractive Indices and Dielectric Constants of Air and its principal Constituents at 24,000 Mc/s. Proc. Phys. Soc. B, 64(10), 862-875.

[22] Tripathi, S. R., et al. 2012. Measurement of Chloride Ion Concentration in Concrete Structures Using Terahertz Time domain Spectroscopy (Thz-TDS). Corrosion Science, 62, 5-10.